ARTICLE IN PRESS

Wear xxx (xxxx) xxx

Contents lists available at ScienceDirect

Wear

journal homepage: http://www.elsevier.com/locate/wear

Automated 3D ferrograph image analysis for similar particle identification with the knowledge-embedded double-CNN model

Shuo Wang, Tonghai Wu [*], Kunpeng Wang

Key Laboratory of Education Ministry for Modern Design and Rotor-Bearing System, Xi'an Jiaotong University, Xi'an, 710049, China

ARTICLE INFO

Keywords:
Wear debris analysis
3D particle classification
Small number of samples
Deep learning

ABSTRACT

Ferrograph-based wear debris analysis (WDA) provides essential information for the root cause analysis of wear failures. However, this technique has been hampered as an intelligent approach by two problems: lack of fault particle samples and conflicts among redundant features. To address this issue, a knowledge-embedded double-CNN model is proposed to identify two representative fault particles: fatigue and severe sliding particles, by using the 3D topographical information. First, a non-parametric CNN network model is constructed with a 2D height map of 3D particle surfaces. The convolution kernels are evaluated to determine identification errors due to the small number of samples. In the refinement stage, four efficient kernels are extracted via the image similarity with the labeled images, which are created based on the physical wear mechanism of the two types of particles. Furthermore, an improved CNN network with six parallel convolution layers is established to handle the feature maps of these kernels for objective particle identification. The proposed model is trained by 20 groups of fault particles and further verified with 10 groups of shuffled particle samples and the network visualization. Validation experiments reveal that discriminative features have contributed to accurately identify all tested fatigue and severe sliding particles.

1. Introduction

Wear is the inevitable failure of tribo-parts in a machine, and the wear failure may exhibit different forms according to its physical mechanism. Unfortunately, it remains blank for directly monitoring ongoing wear failures in a running machine [1,2]. As an indirect technique, wear debris analysis (WDA) plays an exclusive role in wear monitoring. With complex particle morphologies [3–5], typical failures can be identified from particle images such as cutting, fatigue, severe sliding, etc. Over the decades, this promising technique has been driven significantly by intelligent algorithms from the experience-based model to an automated process [6,7]. However, efficiency and accuracy are still restricted due to the small number of available fault particle samples. Moreover, excessive features are constructed for the discrimination of morphologically similar particles, thus introduce conflicts in particle type identification. Prospectively, new breakthrough should be made in intelligent wear particle identification for machine health monitoring (MHM).

The 2D feature-based particle identification model has been widely studied in automatic WDA and accepted in industrial practices. Shape features are combined with clustering algorithms to accurately identify typical particles in distinct characteristics including spherical, rubbing, and cutting particles [8,9]. However, these shape-based methods cannot distinguish particle types in similar contours, such as fatigue and severe sliding particles. To address this issue, more complex 2D texture features have been extracted as inputs to neural networks [10], fuzzy systems [11], or gray theory-based classifiers [8] for comprehensive particle identification. Nevertheless, the recognition accuracy only can be maintained under well-controlled situations. This may be attributed to the morphological characteristics, affected by the oxidation and the material of wear particles, which cannot always be reliably extracted from the gray-scale 2D image.

Correspondingly, researchers begin to focus on 3D features of wear particles in recent years. Particle surfaces are acquired with high-precision techniques like laser scanning confocal microscopy (LSCM) and atomic force microscope (AFM). 3D surface features are extracted [12] and further incorporated in intelligent models including support vector machine (SVM) and BP neural network [13,14]. Similar types of fatigue and severe sliding particles have been well-discriminated with these models, but there are over 200 features constructed to complete

* Corresponding author.
E-mail address: wt-h@163.com (T. Wu).

https://doi.org/10.1016/j.wear.2021.203696
Received 17 August 2020; Received in revised form 31 December 2020; Accepted 31 December 2020
Available online 16 February 2021

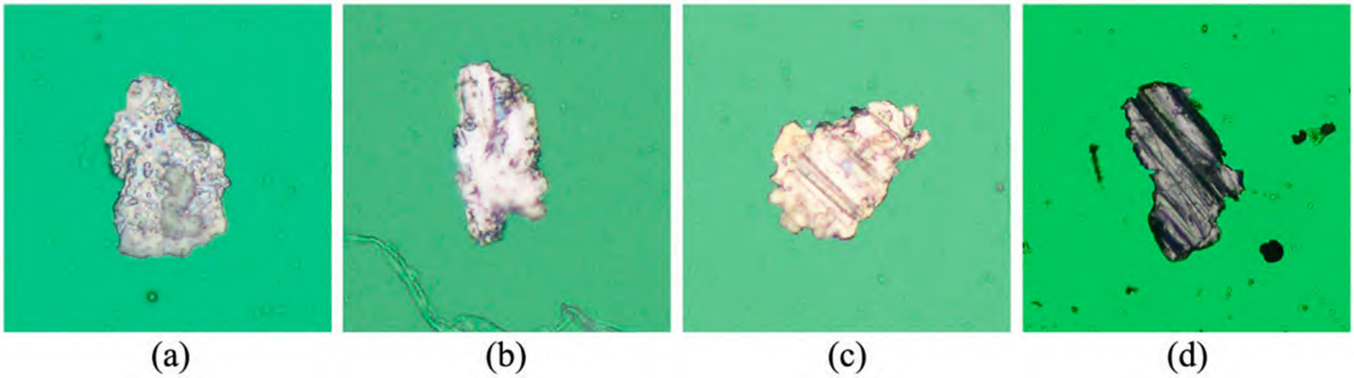

Fig. 1. Fault particle images collected by ferrograph analysis: (a) (b) fatigue particle, (c) (d) severe sliding particle.

this work [15]. With the anticipation of industrial application, excessive operations or features seem to be not desirable. Furthermore, conflicts are unavoidable among the many pieces of evidence for particle recognition.

New non-parametric identification models, especially the convolutional neural network (CNN), are introduced into 2D WDA. 2D images are directly adopted as the network input without manual feature extraction [16], thus, the efficiency of WDA is significantly enhanced [17,18]. However, due to the inherent limitation of the 2D image, these new models are still hindered with low efficiency in identifying similar particle types. Therefore, 3D oriented non-parametric methods seem to be promising solutions. One of the dominant barriers is the small number of training samples. Wear particle samples are highly needed by the training of CNN model, but it is practically difficult to collect sufficient samples from the real wear process. It is because failures do not often occur for a well-designed machine and failures are only due to a narrow range of causes.

To improve the identification of similar particles: fatigue and severe sliding, a knowledge-embedded double-CNN algorithm using a small number of samples is proposed. With the 2D height map of the 3D particle surfaces, the first CNN network is constructed and examined with the visualization to explore the difficulties caused by the limited samples. For further improvement, prior knowledge of particle characteristics is applied to determine four efficient kernels through the image similarity. The second CNN network is established with the feature maps of the four kernels and six parallel convolution layers to locate the difference of similar particle types. This double-CNN framework can increase the importance of critical features of wear particles in the classifier. Considering the small number of fault particle samples, the performance of this methodology is further verified with the network visualization through real wear particles.

The rest of this paper is organized as follows: Section II contains the description of the image properties of object particles, the construction of the CNN-based identification model, and the knowledge-embedded double-CNN model. The verification of the proposed method is given in Section III, followed by discussions in Section IV. The conclusions are presented in Section V.

2. Materials and methods

Three-dimensional surfaces can provide abundant information for WDA, but there are a huge number of constructed features that may not truly represent the wear mechanism, which are redundant for the characterization of similar particles. In addition, the model trained with inadequate samples may result in low identification accuracy. To address this, a knowledge-embedded double-CNN model is proposed for the non-parametric identification of similar 3D fault particles.

2.1. Images of object particles

Reported researches on WDA reveal that different types of particles have their particular morphological characteristics [6–10]. However, with unique generation mechanisms, some of the particles in different categories, such as severe sliding and fatigue, maybe similar in shapes. Severe sliding particles are generated by excessive stress on the surface of friction pairs, while fatigue particles are produced under cyclic contact stress. As shown in Fig. 1, fatigue particle surfaces possess many pits, but parallel scratches exist on severe sliding particles. It can be

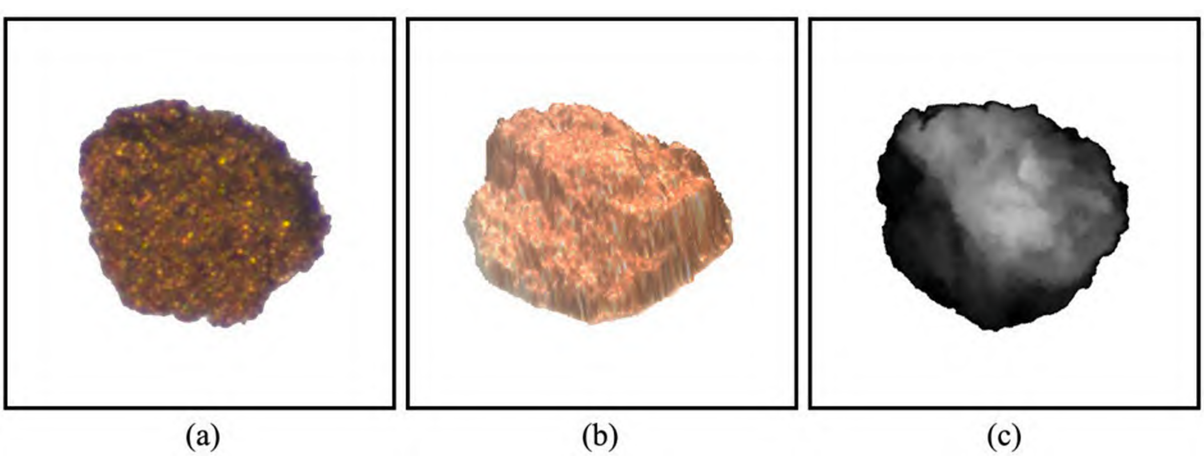

Fig. 2. Image of wear particle in: (a) 2D, (b) 3D topography, (c) 2D height.

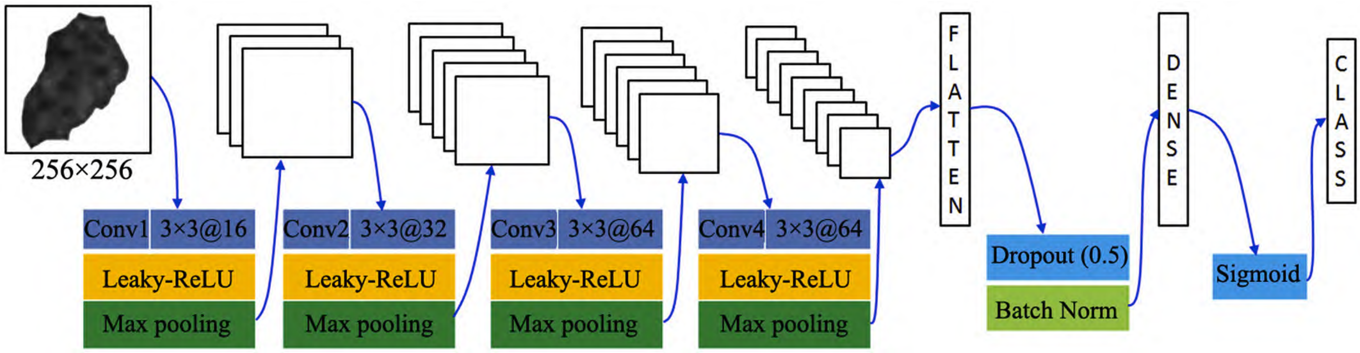

Fig. 3. The framework of the CNN-based particle identification model.

observed that the main difference between the two kinds of particles appears on the surface texture, instead of the size or shape. Therefore, selecting an appropriate information form can promote the identification of similar particles.

As shown in Fig. 2, the particle surface can be described in terms of 2D colored image, 3D morphology, and height transformed image. In contrast, 2D images are usually captured with microscopes [6], which is a standard operation in traditional ferrography analysis. The images composed of color pixels cannot provide morphological information, thus have a low recognition rate for similar particles. 3D surfaces contain a larger amount of morphological data [10], but they are difficult to be handled directly by classification models. Therefore, 3D features have to be constructed and adopted to identify similar particles, but this may cause an insufficient characterization of particle surfaces. Height maps are the transformation from the 3D topography to the 2D datum plane. This image form can reflect the complete surface by the gray change of 2D images. Hence, the height map of particle surfaces is selected as the image form to classify similar particles.

2.2. The construction of CNN-based identification model

A CNN-based model is constructed to deal with the height maps of fatigue particles and severe sliding particles. Because of insufficient training samples, the reliability of the constructed model is analyzed in detail, i.e., its convolution kernels are visualized with their outputs and further explored with class activation maps to show the critical areas of particle images for classification.

2.2.1. Model design

Typical particle analysis can be released from the limitation of artificially-designed features with the CNN model, which provides a non-parametric means for identification [19]. Considering efficiency and accuracy, the CNN-based particle identification model is designed with four convolution layers, as shown in Fig. 3. In this model, the Leaky-ReLU function is employed because it can enhance the nonlinearity of the convolution layer by updating kernels within negative intervals [20]. The max-pooling strategy is introduced to retain texture information. Besides, the dense layer, dropout layer, and batch normalization (BN) layer are added to improve the performance of the model [21,22]. An empirical value (0.5) is selected as the dropout ratio. Finally, the sigmoid function is chosen as the classifier considering its superiority for dichotomous problems.

The loss function can guide the CNN optimization by the error between the predicted result and the real label of training samples. Commonly-used classification loss functions are the mean-variance function and the cross-entropy function [23]. The cross-entropy function, in contrast, is suitable for the image classification. It is because this function can accelerate the training process when combined with the sigmoid classifier. For the two-type identification, the binary cross-entropy (BCE) [24] is chosen for the loss function. It is defined in Equ. (1).

$$log(y_t|y_p) = -\left(y_t \times log(y_p) + (1-y_t) \times log(1-y_p)\right) \tag{1}$$

where, y_t is the real label of the sample, y_p is the probability of $y_t = 1$ of the sample.

2.2.2. Model training

Gradient Descent (GD) algorithm is often applied in training the CNN [25]. However, it has low training efficiency due to the fixed learning rate and a one-time weight update for all kernels. In view of this, an effective method has been developed with an adaptive learning rate, that is, Adam algorithm, which can calculate the learning rate from the mean value of the first-order and second-order moments [26]. Therefore, this effective training method is adopted here.

As emphasized, the image samples of fault particles are difficult to obtain from real machines. With the standard ferrograph analysis, only 30 fatigue and 30 severe sliding wear particle images are collected from wear test oils. Twenty pairs of images are used as training samples and the rest are test samples. The CNN-based particle identification model is trained by the Adam trainer with a learning rate of 0.0001 and the iteration is 200. The CNN model converges rapidly as the number of iterations increases and stabilized after the 25th iteration. It may be concluded that this designed CNN structure can effectively deal with trained particle samples under the Adam optimization algorithm. Ten sets of fatigue and severe sliding particles are applied to test the trained model. The CNN-based model can identify all tested particles with absolute accuracy. Part of the result is shown in Table 1.

2.2.3. Kernel visualization

With multiple convolution layers, the trained CNN model can extract the overall features from wear particle images. However, salient features such as boundaries would be strengthened due to dramatic gray-scale changes. Comparatively, the surface features of object particle images

Table 1
The identification results of tested fault particles with the knowledge-embedded double-CNN model (Note: F_* represents the tested fatigue particle, while S_* is for the severe sliding particle).

Type	F_1	F_2	F_3	F_4	F_5	S_1	S_2	S_3	S_4	S_5
Fatigue	100%	100%	100%	100%	100%	0%	0%	0%	0%	0%
Sliding	0%	0%	0%	0%	0%	100%	100%	100%	100%	100%

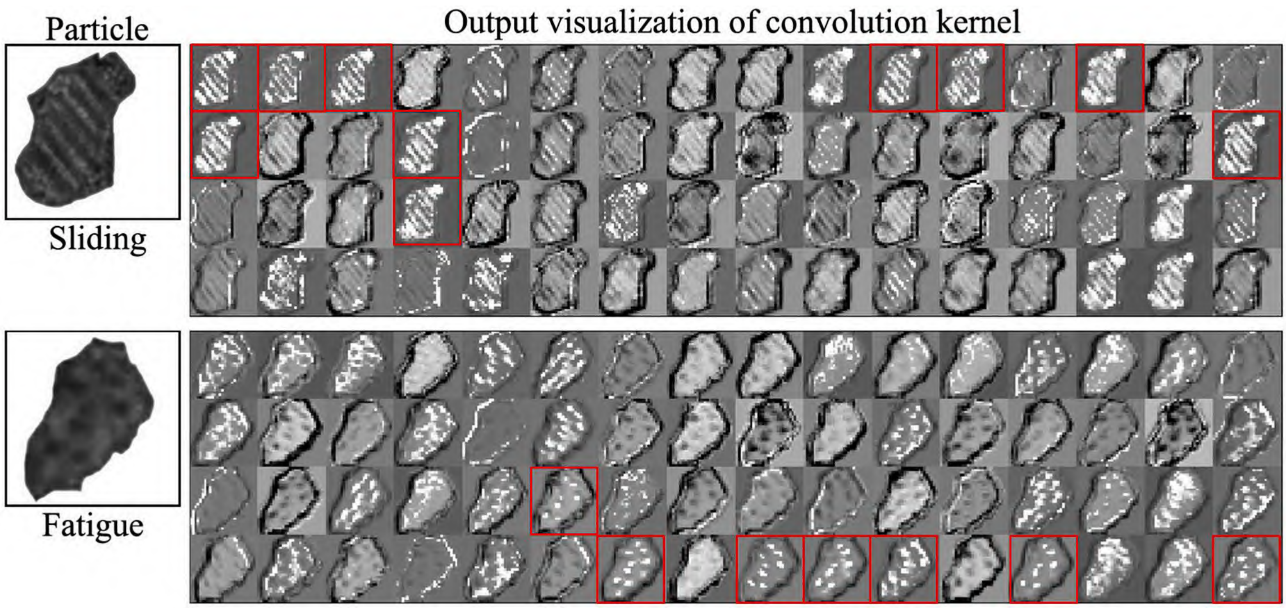

Fig. 4. Feature maps of Conv4 convolution kernels in the constructed CNN model (Note: Feature maps with critical features are shown in red bounding boxes). (For interpretation of the references to color in this figure legend, the reader is referred to the Web version of this article.)

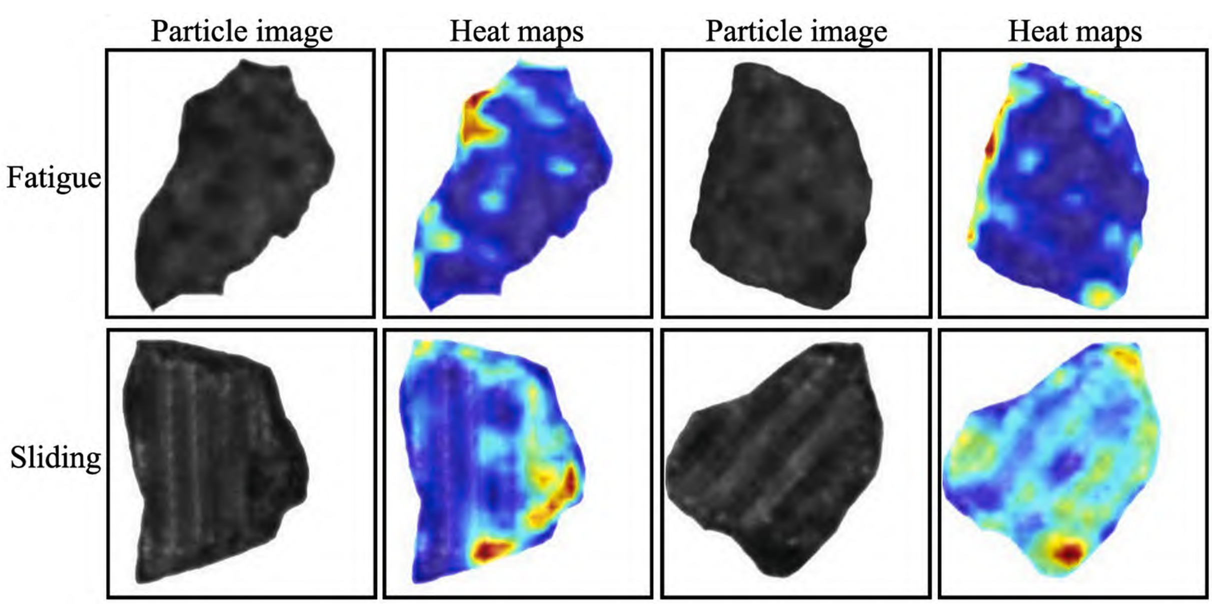

Fig. 5. Class activation maps for Conv4 in the constructed CNN model.

are weak, thus may be weakened in the convolution process. This would be aggravated when training samples are insufficient as happened in this work. Therefore, convolution kernels in the constructed CNN model are further visually inspected with their feature maps and class activation maps.

2.2.3.1. Feature maps of convolution kernels. Different convolution kernels focus on different characteristics, thus the evolution of the feature extraction can be traced by checking the output of convolution layers, i.e. feature maps. Since the convolution layer Conv4 is closely connected with the classifier, its kernels are visualized with the fatigue particle and the severe sliding particle images. The feature maps are shown with two 3×18 sub-image matrixes in Fig. 4.

As can be seen from Fig. 4, different morphological features are extracted with different convolution kernels. Most importantly, the Conv4 layer has extracted a small number of discriminative features for characterizing typical particles. These include parallel scratches for severe sliding particles and pits for fatigue particles. However, further checks show that the edge features are over-emphasized as compared with the surface features. This may introduce invalid identifications using unnecessary features rather than the essential ones. Further evaluations are carried out to identify the dominant elements for the final classification.

2.2.3.2. Class activation maps. The Grad-CAM can provide class activation maps by summing all feature maps with the gradient of the convolution layer [27,28]. As the convolution layer is closely connected with the classifier, the Conv4 layer is also processed with Grad-CAM to locate the discriminative area for classification. The importance of a given kernel category is

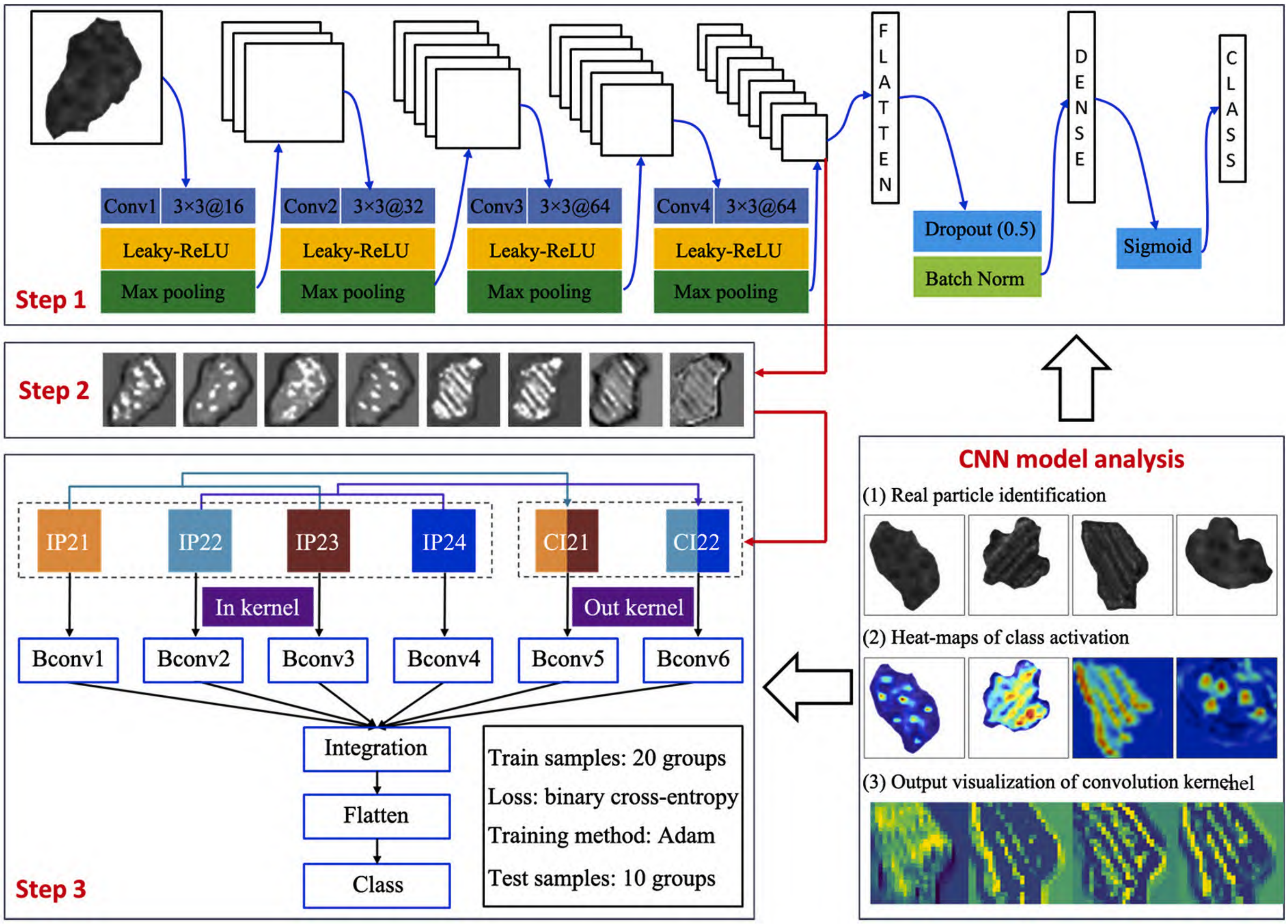

Fig. 6. Framework of the knowledge-embedded double-CNN model for identifying 3D fault particles with a small number of samples.

$$Y^c = \sum_k \omega_k^c \frac{1}{Z} \sum_i \sum_j A_{ij}^k \tag{2}$$

where, Z is the number of pixels in the feature map, Y^c is the importance of given category c, and A_{ij}^k refers to the activation at the location (i,j) of the feature map A^k, ω_k^c is the weight connecting the k^{th} feature map with the c^{th} class.

Fig. 5 shows a collection of class activation maps extracted by Grad-CAM. As can be seen, discriminative elements for both severe sliding and fatigue particle images mostly exist on particle edges rather than on surface textures. It can be generalized that the constructed model cannot achieve good performances for fatigue and severe sliding particles with these features. For the high identification accuracy achieved in Section 2.2.2, this may due to the situation that limited training samples may possess differences on the boundary for the two kinds of fault particles, so the CNN model is mistakenly trained to adapt to the edge features as the discriminative feature. However, the recognition accuracy will be sharply reduced in real-world applications, after all, the kernel adopts useless features.

2.3. Knowledge-embedded double-CNN model

As mentioned before, the surface features including distributed pits and parallel scratches, are critical for identifying fatigue and severe sliding particles. These surface features are weak but still can be distinguished from some of feature maps, as shown in Fig. 4. If these efficient feature maps can be chosen and applied to construct a new CNN model, the efficiency of the particle identification model can be enhanced by increasing the weight of discriminative features. Therefore, a knowledge-embedded double-CNN model is proposed with the framework shown in Fig. 6.

Three steps are involved in model construction. First, the CNN model in Section 2.2 is adopted as the first network to extract high-level features of fault particle samples. Second, masked images are created with the empirical knowledge to characterize the surface features and they are further applied to select the efficient kernels from the Conv4 layer of the first CNN network. In the final step, the second CNN network is constructed with six parallel convolution layers to deal with the feature maps of the four selected kernels, and output the final particle type.

The first CNN network has been described in detail in Section 2.2, and the visualization results show that its convolution kernels can provide typical feature maps for fault particles. Further details of the procedure are presented in the sections below.

2.3.1. Knowledge-embedded efficient convolution kernel filtering

To select efficient kernels from the first CNN network, the filtering of convolution kernels is carried out, which involves (1) image enhancement for feature maps, (2) knowledge characterization of typical particles, and (3) efficient convolution kernel filtering.

2.3.1.1. Image enhancement for feature maps. As seen in Fig. 4, the surface features of typical particles can be observed from feature maps. However, there is excessive noise in these maps. To enhance the dominant feature, threshold segmentation is introduced to eliminate the disturbance information in the gray-scale feature maps. With the

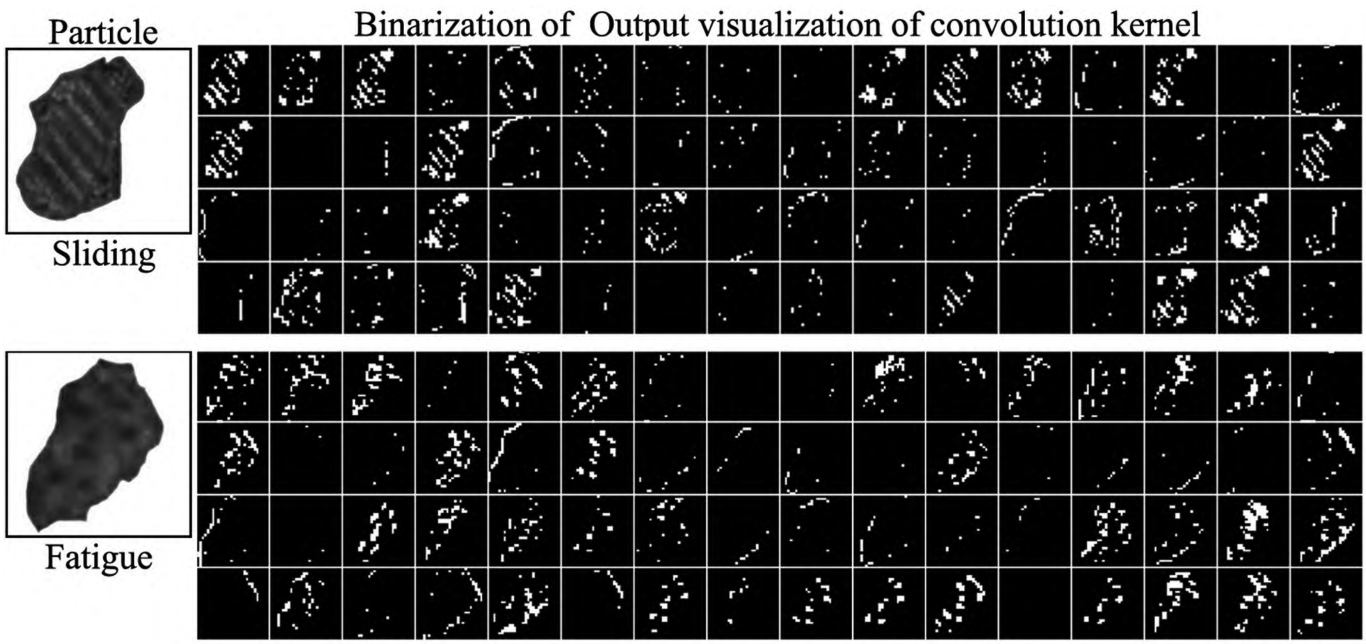

Fig. 7. Threshold segmented feature maps for dominant feature enhancement.

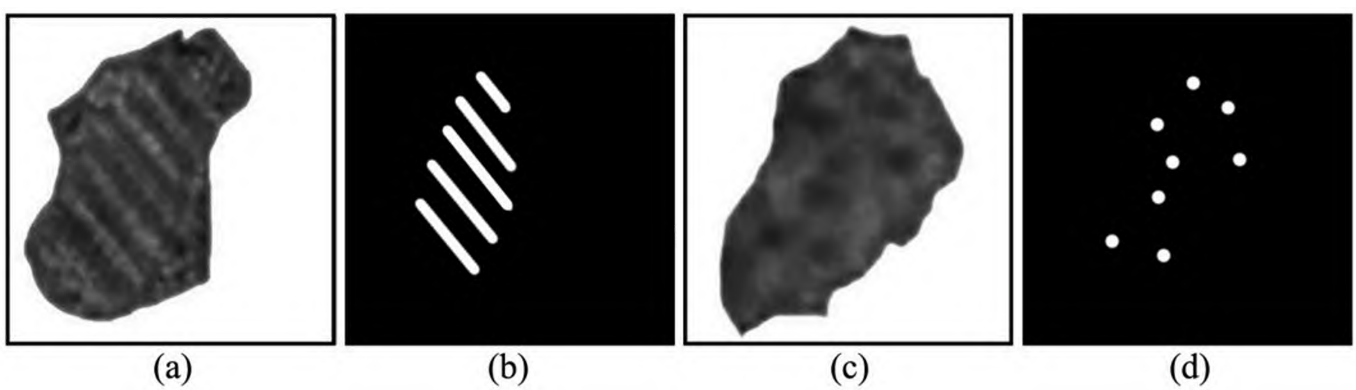

Fig. 8. Knowledge-based masks of typical particles: (a) severe sliding particle, (b) masked parallel scratches, (c) fatigue particle, (d) masked pits.

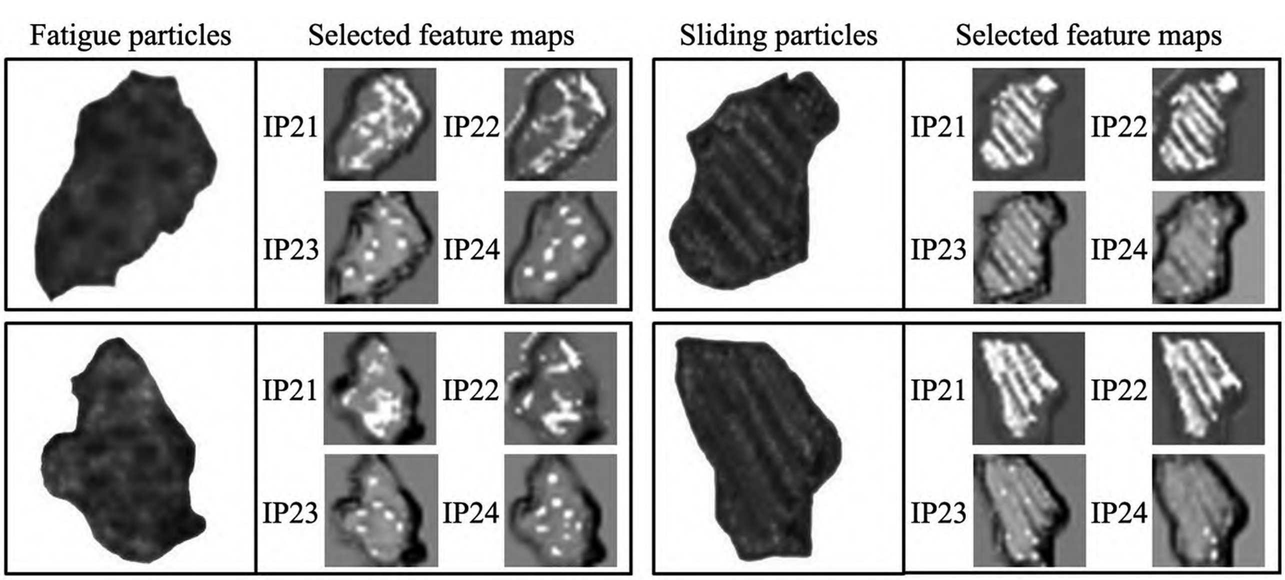

Fig. 9. Feature maps of the selected four convolution kernels.

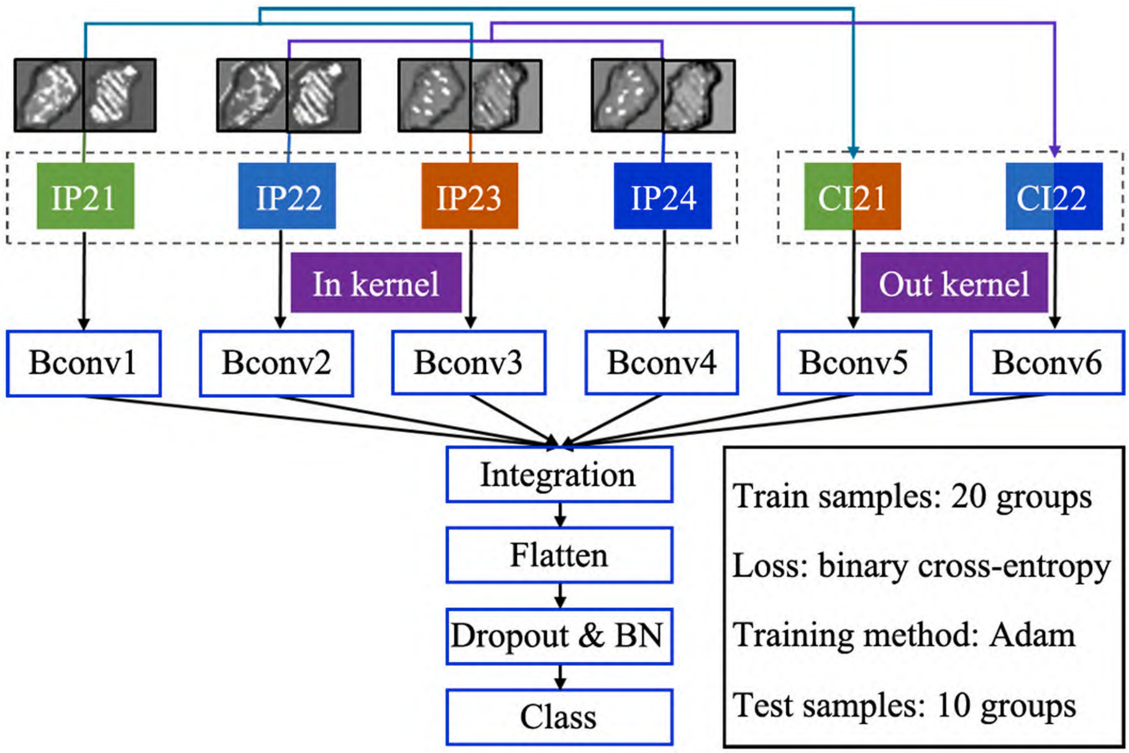

Fig. 10. The framework of the second CNN network with four feature maps.

threshold (230), the feature maps are processed to be the binary one, which only contains the concerned region and black background, as shown in Fig. 7. This would facilitate the selection of efficient convolution kernels and provide critical morphological features for typical particles.

2.3.1.2. Knowledge characterization of typical particles. Even with the empirical knowledge of typical features of object fault particles as described in Section 2.1, it is not easy to automatically select efficient kernels with high efficiency. After all, the experience-based ferrograph could not provide a unique standard for these similar but diverse features. That means empirical knowledge should be involved to mask the critical features in the particle image. With the particle generation [7–9], two kinds of masks are created for the two types of particles, as shown in Fig. 8. The height maps of fatigue and severe sliding particles are simplified by masking pits or parallel scratches in white, and the background is shown in black.

2.3.1.3. Convolution kernel selection. With the above two processes, the feature maps and the knowledge-based masked images have been obtained in binary format, which contains rich structure information of key features but less color and gray-scale information. By checking the structural similarity with these two images, the object kernels can be selected. Compared with the structural similarity (SSIM) and the Hash perception algorithms [29,30], cosine similarity (CS) [31] is calculated based on the structural features of the image without color information. Therefore, the CS is adopted in this work, which converts each image into a vector and calculates the cosine angle of the two vectors as the image similarity.

With the CS similarity measure, four convolution kernels are selected from the first CNN network. As shown in Fig. 9, the feature maps of these convolutional kernels are acquired by inputting fault particle images. The images IP21 and IP22 describe the characteristics of severe sliding particles, while IP23 and IP24 represent the critical features of fatigue particles.

2.3.2. The second CNN construction with selected kernels

The feature maps are unique that it can only describe one particle type, such as IP21 in Fig. 9 that is only for severe sliding particles. To make full use of the feature maps of the four selected kernels, a CNN model with four inputs is constructed, in particular, it contains six parallel convolutional layers. Its structure is shown in Fig. 10.

After processed by the first CNN network, the selected feature maps are already high-level features. Only one single convolution layer is introduced for each input in the second CNN network. Maps IP21 and IP22 are the inputs to convolution layers Bconv1 and Bconv2, respectively. Convolution layers Bconv3 and Bconv4 are respectively fed with maps IP23 and IP24. To prevent the CNN model from relying on a single convolution kernel, the feature maps of fatigue and severe sliding particles are mixed and inputted into a new convolution layer. Specifically, the input of the convolution layer Bconv5 is the mixed feature maps of IP1 and IP3, and the Bconv6 layer is inputted with the mixed maps of IP2 and IP4. With this framework, the constructed model can learn the difference between similar particles in and between convolution kernels. Each convolution layer contains 32 convolution kernels with a size of 3×3. The six convolution layers are integrated and inputted to the flatten layer.

Similar to the first CNN network presented in Section 2.2, Dropout and BN layers are also introduced to enhance the second CNN network. The sigmoid function and the binary cross-entropy loss are still adopted as the classifier and the loss function. Twenty sets of feature maps of fatigue particles and severe sliding particles are selected as training samples. The second CNN network is trained with the Adam algorithm (learning rate 0.0001). The training iteration is set to 200, and the training process is shown in Fig. 11. The recognition accuracy and training loss of the second CNN network converge rapidly and stabilized after the 50th iteration. This indicates that the designed CNN structure is effective in processing the feature maps of the four selected kernels through six parallel convolution layers.

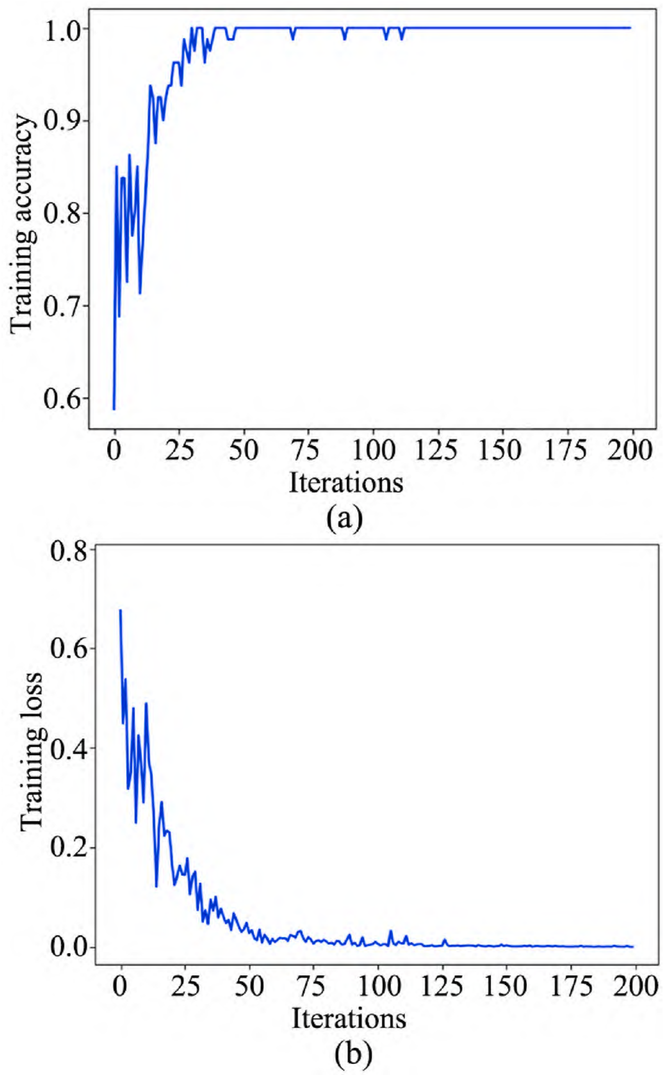

Fig. 11. Training process of the constructed CNN model with four feature maps: (a) training accuracy, (b) training loss.

3. Verification

The knowledge-embedded double-CNN model is established with the first and second CNN networks, which are connected by the efficient convolution kernel filtering. The performance of this method is verified with the particle identification accuracy and the network visualization. The height maps of wear particles are inputted into the first CNN network to obtain four feature maps, and then these maps are handled with the second CNN network to obtain the final identification results.

3.1. Real particle identification

To acquire tested wear particles, the wear experiment is carried out with a four-ball tester, which is a commonly-used wear test rig [32]. The friction pair is composed of four steel balls manufactured by the carbon chromium bearing steel (GCr15). By specifying loads and rotation speeds, the friction pair can be worn and generate different types of wear particles. With the ferrograph technology, ten groups of severe sliding particles and fatigue particles are collected from the lubricant oil of the four-ball tester. The surfaces of these particles are obtained with the 3D reconstruction method [4] and then transformed into height maps as the tested samples. With the first and second CNN networks, the classifier outputs the recognition probability of tested particles. Examples of input images of the two CNN networks are displayed in Fig. 12. The developed double-CNN network can accurately identify all tested particles. Part of recognition results are shown in Table 2.

3.2. Visualization of the output convolution kernel

The extracted features of convolution kernels can be explored with their output. The integration layer of the second CNN network is closely connected with the final classifier, thus it is visualized with the severe sliding particle and the fatigue particle, as shown in Fig. 12. It can be observed that most of the feature maps are extracted around the key features of severe sliding or fatigue particle images. The convolution kernels of the integration layer pay more attention to surface features than the Conv4 layer in the first CNN network, which can be concluded from the number of feature maps containing surface textures in Figs. 4 and 12. Therefore, the constructed model can extract more distinguished features for severe sliding and fatigue particles through efficient convolution kernel filtering and the double-CNN structure.

3.3. Class activation maps

Similar to Section 2.2, class activation maps are adopted to show the key area used for particle classification. The second CNN network determines the final identification, thus all convolution layers of the second CNN network are visualized with Grad-CAM, as shown in Fig. 12. It can be seen that the results are consistent with the training samples of each convolution layer. For the fatigue particle, Bconv1 and Bconv2 layers extract no significant regions, while the distinguishing regions of layers Bconv3 and Bconv4 are the particle pits, which are also located by the mixed layers of Bconv5 and Bconv6. For the severe sliding particles, the significant areas acquired by convolution layer Bconv1 and Bconv2 are parallel scratches, while there is no distinctive area in convolution layers Bconv3 and Bconv4. Part of the key features is extracted by mixed layers Bconv5 and Bconv6. As the layer is closely connected with the classifier, the integration layer adopts the surface pits for the fatigue particle and parallel scratches for the severe sliding particle. Therefore, the knowledge-embedded double-CNN model is able to adopt typical features to identify similar particles.

Considering the verification results, the knowledge-embedded double-CNN model can be regarded as a useful model for identifying 3D fault particles with a small number of samples. Moreover, this model can be applied to identify severe sliding particles and fatigue particles.

4. Discussion

A knowledge-embedded double-CNN method is developed for identifying the 3D surfaces of similar wear particles with a small number of samples. The method involves image forms for identification, the first CNN network, efficient convolution kernel filtering, and the second CNN network. The proposed method achieves an effective identification for similar particles by embedding the empirical knowledge into the CNN-based identification model. The comparison between the proposed method and other methods is given below.

The combination of 2D surface textures and intelligent methods [6, 17] (including the parameter-based and non-parametric models) have promoted the automation of wear particle identification. However, 2D particle images only provide the color information rather than the surface morphology, which may fail to character similar particles. When compared with 3D WDA methods [11], the advantage of the proposed identification method is that the CNN model directly adopts the change of 3D surface heights as the input. This approach can avoid the loss of surface information due to artificially-designed features. In addition, typical particles are difficult to be collected from operating machines, which will lead to insufficient training of the CNN network. To address this issue, double CNNs are introduced. Empirical knowledge is adopted to select four efficient convolution kernels from the first CNN network,

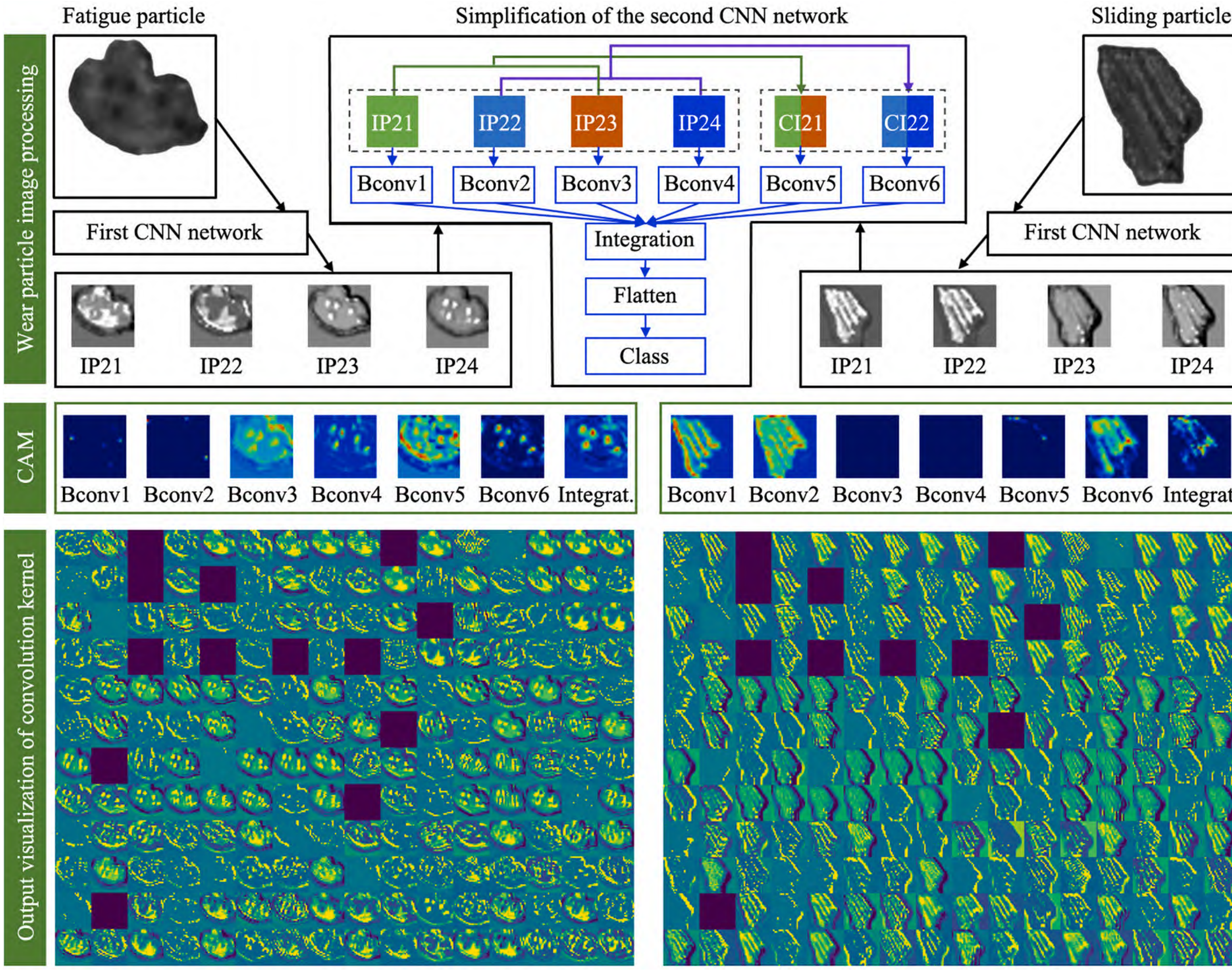

Fig. 12. Validation for knowledge-embedded double-CNN fault particle identification model (Note that CAM represents the class activation map).

Table 2
The identification results of tested fault particles with the knowledge-embedded double-CNN model (Note: F_* represents the tested fatigue particle, while S_* is for the severe sliding particle).

Type	F_1	F_2	F_3	F_4	F_5	S_1	S_2	S_3	S_4	S_5
Fatigue	100%	100%	99.9%	99.7%	100%	0%	1.1%	1.7%	0%	0%
Sliding	0%	0%	0.1%	0.3%	0%	100%	98.9%	98.3%	100%	100%

and then the output maps of these kernels are inputted into the second CNN network to obtain the final identification. With this structure, the importance of the valid features is increased to ensure that the CNN network can realize identification using a small number of samples. Therefore, the proposed knowledge-embedded double-CNN method can be considered as an effective means for WDA.

For industrial applications, rubbing, spherical, and cutting particles will be first recognized with their typical shape characteristics [7], and the remaining morphologically-similar fatigue and severe sliding particles will be identified by the proposed knowledge-embedded double-CNN method. By this hierarchical identification strategy, the identification accuracy of typical particles can be significantly improved. This work will contribute toward enhancing the wear state analysis for machine condition monitoring.

5. Conclusions

A knowledge-embedded particle identification model is proposed and applied to identify fatigue and severe sliding wear debris. The developed double-CNN model uses the height maps of particle surfaces as the input, and its main features include:

(1) By selecting CNN structures and optimization approaches, a CNN model is constructed to extract high-level features from wear particle surfaces;
(2) Based on the empirical knowledge, four efficient convolution kernels are selected via the similarity for the typical particle description;

(3) Using the efficient feature maps, a CNN-based identification model with four inputs and six parallel convolution layers is established to distinguish similar particles.

This investigation offers an insight into the efficiency in the automatic classification of similar wear particles. This work will contribute toward enhancing the analysis of machine wear states.

CRediT authorship contribution statement

Shuo Wang: Methodology, Software, Validation,Writing-Original draft preparation. **Tonghai Wu:** Supervision, Writing-Reviewing and Editing. **Kunpeng Wang:** Investigation.

Declaration of competing interest

The authors declare that they have no known competing financial interests or personal relationships that could have appeared to influence the work reported in this paper.

Acknowledgement

This work is supported by the National Natural Science Foundation of China (No. 51975455 and No. 51675403). The authors gratefully acknowledge the support of K.C. Wang Education Foundation.

References

[1] N. Gebraeel, A. Elwany, J. Pan, Residual life predictions in the absence of prior degradation knowledge, IEEE Trans. Reliab. 58 (1) (2009) 106–117.
[2] C. Huang, X. Yin, H. Huang, Y. Li, An enhanced deep learning-based fusion prognostic method for rul prediction, IEEE Trans. Reliab. (2019) 1–13.
[3] T. Wu, Y. Peng, H. Wu, X. Zhang, J. Wang, Full-life dynamic identification of wear state based on on-line wear debris image features, Mech. Syst. Signal Process. 42 (1) (2014) 404–414.
[4] S. Wang, T. Wu, L. Yang, N.M. Kwok, T. Sarkodiegyan, Three-dimensional reconstruction of wear particle surface based on photometric stereo, Measurement 133 (2019) 350–360.
[5] W. Hong, S. Wang, M. Tomovic, H. Liu, J. Shi, X. Wang, A novel indicator for mechanical failure and life prediction based on debris monitoring, IEEE Trans. Reliab. 66 (1) (2017) 161–169.
[6] J. Wang, G. Wang, L. Cheng, Texture extraction of wear particles based on improved random hough transform and visual saliency, Eng. Fail. Anal. 109 (2020) 104299.
[7] S. Wang, T. Wu, T. Shao, Z. Peng, Integrated model of bp neural network and cnn algorithm for automatic wear debris classification, Wear (2019) 1761–1770.
[8] J. Wang, X. Wang, A wear particle identification method by combining principal component analysis and grey relational analysis, Wear 304 (1) (2013) 96–102.
[9] W. Yuan, K. Chin, M. Hua, G. Dong, C. Wang, Shape classification of wear particles by image boundary analysis using machine learning algorithms, Mech. Syst. Signal Process. 72 (2016) 346–358.
[10] Z. Peng, T.B. Kirk, Computer image analysis of wear particles in three-dimensions for machine condition monitoring, Wear 223 (1) (1998) 157–166.
[11] Z. Peng, T.B. Kirk, Wear particle classification in a fuzzy grey system, Wear 225 (2) (1999) 1238–1247.
[12] J. Song, F. Chen, Y. Liu, S. Wang, X. He, Z. Liao, X. Mu, M. Yang, W. Liu, Z. Peng, Insight into the wear particles of peek and cfrpeek against uhmwpe for artificial cervical disc application: morphology and immunoreaction, Tribol. Int. 144 (2020) 106093.
[13] G.P. Stachowiak, G. Stachowiak, P. Podsiadlo, Automated classification of wear particles based on their surface texture and shape features, Tribol. Int. 41 (1) (2008) 34–43.
[14] J. Wu, Z. Peng, Investigation of the geometries and surface topographies of uhmwpe wear particles, Tribol. Int. 66 (2013) 208–218.
[15] B. Xu, G. Wen, Z. Zhang, F. Chen, Wear particle classification using genetic programming evolved features, Lubric. Sci. 30 (5) (2018) 229–246.
[16] D. Han, Q. Liu, W. Fan, A new image classification method using cnn transfer learning and web data augmentation, Expert Syst. Appl. 95 (2018) 43–56.
[17] P. Peng, J. Wang, Wear particle classification considering particle overlapping, Wear (2019) 119–127.
[18] Y. Peng, J. Cai, T. Wu, G. Cao, N.M. Kwok, S. Zhou, Z. Peng, A hybrid convolutional neural network for intelligent wear particle classification, Tribol. Int. 138 (2019) 166–173.
[19] F.D. Santos, P.F. Pimenta, C. Lunardi, L.K. Draghetti, L. Carro, D. Kaeli, P. Rech, Analyzing and increasing the reliability of convolutional neural networks on gpus, IEEE Trans. Reliab. 68 (2) (2019) 663–677.
[20] B. Xu, N. Wang, T. Chen, M. Li, Empirical Evaluation of Rectified Activations in Convolutional Network, (arXiv: Learning).
[21] N. Srivastava, G.E. Hinton, A. Krizhevsky, I. Sutskever, R. Salakhutdinov, Dropout: a simple way to prevent neural networks from overfitting, J. Mach. Learn. Res. 15 (1) (2014) 1929–1958.
[22] S. Ioffe, C. Szegedy, Batch Normalization: Accelerating Deep Network Training by Reducing Internal Covariate Shift, (arXiv: Learning).
[23] K. Wang, A. Kumar, Cross-spectral iris recognition using cnn and supervised discrete hashing, Pattern Recogn. 86 (2019) 85–98.
[24] L. Liu, A. Rahimpour, A. Taalimi, H. Qi, End-to-end binary representation learning via direct binary embedding, in: International Conference on Image Processing, 2017, pp. 1257–1261.
[25] J.C. Duchi, E. Hazan, Y. Singer, Adaptive subgradient methods for online learning and stochastic optimization, J. Mach. Learn. Res. 12 (2011) 2121–2159.
[26] D. P. Kingma, J. Ba, Adam: A Method for Stochastic Optimization, (arXiv: Learning).
[27] B. Zhou, A. Khosla, A. Lapedriza, A. Oliva, A. Torralba, Learning deep features for discriminative localization, in: Computer Vision and Pattern Recognition, 2016, pp. 2921–2929.
[28] R.R. Selvaraju, M. Cogswell, A. Das, R. Vedantam, D. Parikh, D. Batra, Grad-cam: visual explanations from deep networks via gradient-based localization, in: Proceedings of the IEEE International Conference on Computer Vision, 2017, pp. 618–626.
[29] H. Zhao, O. Gallo, I. Frosio, J. Kautz, Loss Functions for Neural Networks for Image Processing, 2015.
[30] K. Zhang, J. Wang, B. Hua, L. Lu, Dhash: a cache-friendly tcp lookup algorithm for fast network processing, in: IEEE Conference on Local Computer Networks, 2013, pp. 484–491.
[31] Z. Wang, A.C. Bovik, H.R. Sheikh, E.P. Simoncelli, Image quality assessment: from error visibility to structural similarity, IEEE Trans. Image Process. 13 (4) (2004) 600–612.
[32] S. Wang, T. Wu, H. Wu, N. Kwok, Modeling wear state evolution using real-time wear debris features, Tribol. Trans. 60 (6) (2017) 1022–1032.